特集 10　—研究速報—　　UDC 669.13.046.56-492 : 621.762 : 621.73

POWDER FORGING OF DECARBONIZED CAST IRON POWDER

脱炭鋳鉄粉の粉末鍛造

Takeo NAKAGAWA* and Feng-Shuh DAI**

中川威雄・戴豊樹

1. Introduction

The main advantage of substituting powder forging for other manufacturing process is that there is an economical saving in materials and subsequent machining. Most of the technical problems have been solved by continuous research and development works which have been done in the past ten years. But powder forging is still unable to produce so many mechanical parts in an economical way. To overcome this higher manufacturing cost problem of the powder forged products, the conversion from conventional metal powder to swarf powder has been tried by the authors [1),2),3)] and the other researchers.[4),5)]

The aim of the present work is to develope the powder forging process with high carbon steel powder which is obtained by extracting free graphite flakes from grey cast iron swarf powder. This paper deals with the whole powder forging process including decarbonizing and the mechanical properties of the decarbonized cast iron powder forged products.

2. Decarbonized Cast Iron Powder

The grey cast iron contains 3.55% carbon totally and approximately 2.5～3% carbon exists in the state of free graphite flakes. Decarbonizing is carried out by extracting these free graphite flakes from the cast iron powder which is understood as a mixture of free graphite flakes and high carbon steel particles.

Fig. 1 illustrates diagrammatically the manufacturing process of decarbonized cast iron powder from machining swarf. Pulverizing of cast iron swarf is done by a conventional hammer mill. Since the cast iron machining swarf is weak and brittle, it can be crushed easily to a micro-mesh powder. The difference in specific gravity between the graphite flakes and the high carbon steel particles is great, thereby it facilitates the extraction of carbon from cast iron powder by a cyclone machine which is connected to the

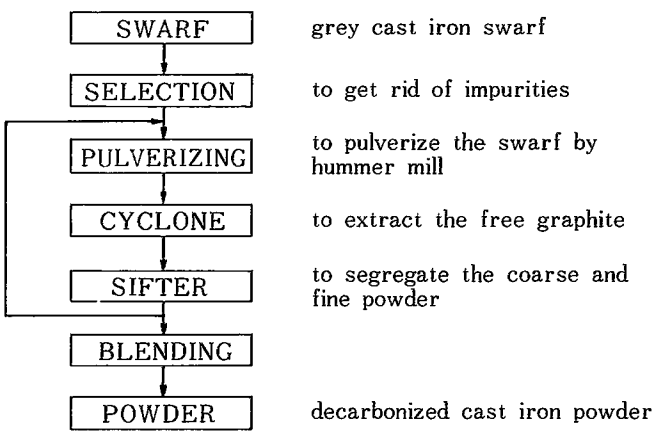

Fig. 1　Manufacturing process of the decarbonized cast iron powder from swarf.

* Dept. of Mechanical and Naval Architecture, Composite Materials Research and Development Center, Institute of Industrial Science, University of Tokyo.
** Dept. of Mechanical and Naval Architecture, Institute of Industrial Science, University of Tokyo.

crushing machine. After sieving by a sifter, the coarse and very fine powder among the pulverixed powder is segregated in order to remove the higher amount of carbon included inside.

As the decarbonized cast iron powder is not subjected to any annealing or reducing heat treatment, the cost of the powder is almost the same as that of cast iron powder used for sintering, which is about one third of the price of iron powder.

Table 1 compares the chemical compositions of grey cast iron and decarbonized cast iron. The abovementioned decarbonizing process reduces the carbon content by about 2% to 1.4%.

Table 2 shows the characteristics of decarbonized cast iron powder. Flowability is a little improved by decarbonizing and the mesh size distributions are not so

Table 1 Chemical compositions of parent cast iron and decarbonized cast iron powder.

Material	Chemical compositions (%)					
	C	Si	Mn	P	S	Fe
Parent cast iron	3.55	2.69	0.46	0.13	0.05	bal.
Decarbonized cast iron	1.41	3.02	0.47	0.05	0.05	bal.

Table 2 Characteristics of the decarbonized cast iron powder.

Apparent density (g/cc)	2.22
Flow rate (sec/50g)	24.3
Powder size distributions	%
48 – 65	4.2
65 – 100	19.6
100 – 150	23.5
150 – 200	22.1
200 – 270	13.6
270 –	17.0

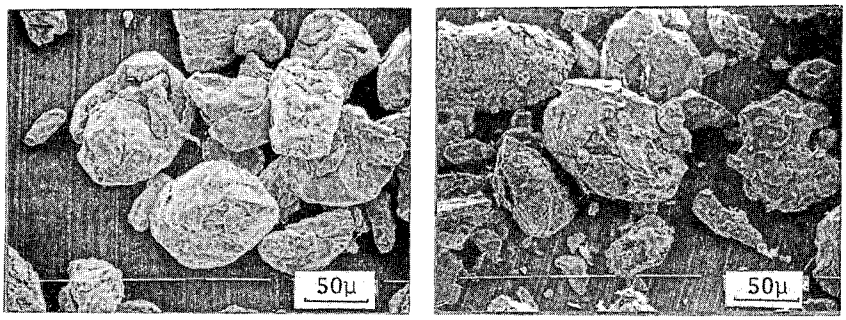

(a) decarbonized cast iron powder　　(b) cast iron powder

Fig. 2 The configurations of decarbonized cast iron powder and cast iron powder.

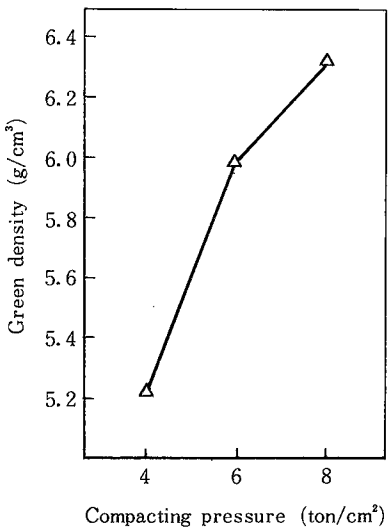

Fig. 3 Relation between compacting pressure and density.

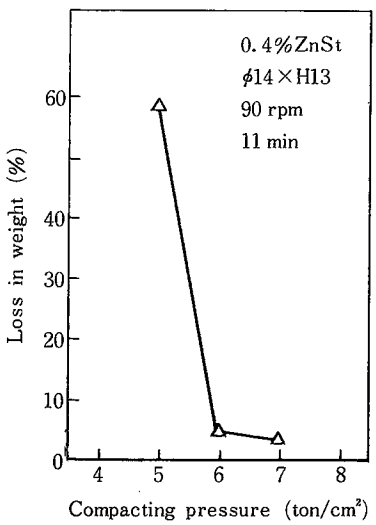

Fig. 4 Result of rattler test.

different from those of conventional iron powder.

The photographs in Fig. 2 show the configurations of decarbonized cast iron powder along with the cast iron powder. Machining swarf originally has a more ragged and irregular surface. Through the pulverization by the hammer mill, the shape becomes a little rounded.

Fig. 3 shows the relation between the compacting pressure and the density of powder preform. Fig. 4 indicates the strength of the green compact. From this result, it can be seen that the compacting pressure for making the preform should be more than 6 ton/cm^2.

3. The Powder Forging of Decarbonized Cast Iron Powder

In order to carry out the powder forging experiment, the dimensions of preform and forged product were arranged as in Fig. 5. The compacting pressure selected for the preform was 6 ton/cm^2. The preform and the forged product are pressed in the same direction. The hot densification type of forging is adopted, due to the lack of plastic flowability in cast iron.

The powder forging experiment with decarbonized cast iron powder involves the following steps: (1) compacting, (2) sintering, (3) forging, (4) reheating. Fig. 6 illustrates the time-temperature relation of this forging process. In the first step, the preform was heated in a furnace with ammonium cracking gas atomospher, by preheating at 800°C and sintering at 1150°C for 30 minutes. In the next step, the heated preform is forged in the air by 12 ton/cm^2 forging pressure. In the forging, the die is preheated at 210°C and lubricated with a colloidal dispersion of graphite in water. Afterwards the forged test piece is returned to the furnace and reheated at 1150°C for one and half hours.

In this process, the reheating step which is not usually adopted in the conventional powder forging process can not be neglected. This is because, reheating was found to be very efficient in the preliminary experiment, especially for cast iron powder with it's strong sensitivity for sintering temperature, for obtaining sufficinet mechanical properties.

The density of forged product is measured to be 7.31 ~ 7.41 g/cm^3, while the preform density is 5.97 ~ 6.05 g/cm^3. This shows that the forged product is in full density as no pore can be found in an examination of their microstructures.

4. Mechanical Properties of the Powder Forged Product

The forged products were subjected to various heat-treatments for checking their mechanical properties. The details of the heat-treatment conditions and the mechanical properties of forged products are presented in Table 3. The forged test piece is almost the same size as the standard Charpy impact test specimen. The tensile test piece is obtained by machining the forged product. In this table, "air cooling" means the condition of the forged product after reheating. In regards to the annealed condition of the forged product, the tensile strength decreases to 53 kg/mm^2 but its elongation approaches 12.7%. By austempering, its strength reaches 107 kg/mm^2 and Charpy value is 6.2 kg·m/cm^2. Of

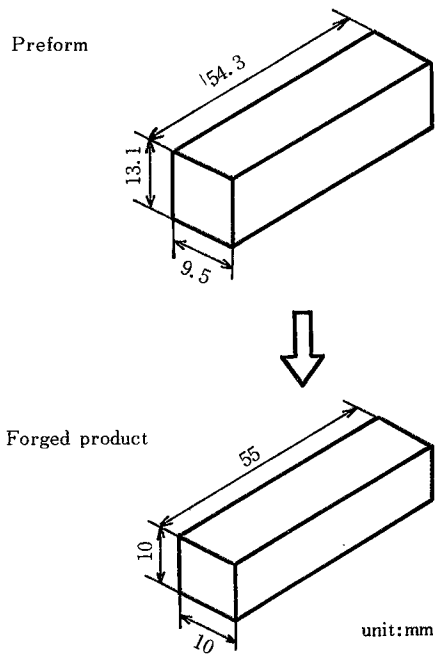

Fig. 5 Dimensions of preform and powder forged product.

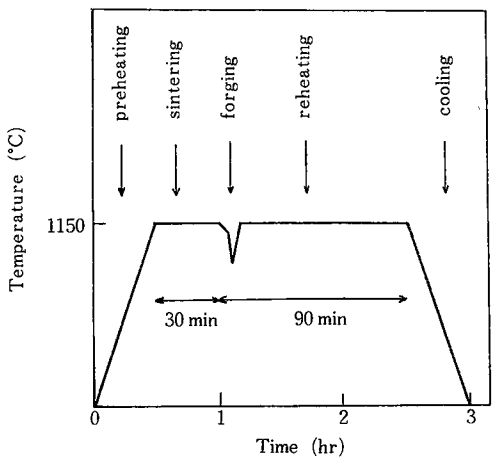

Fig. 6 The forging process of decarbonized cast iron powder.

Table 3 Mechanical properties of forged products of decarbonized cast iron powder under various heat-treatment conditions.

	Heat-treatment	Hardness (Rockwell)	T.S. (kg/mm^2)	Elong. (%)	Charpy impact value w/o notch (kg·m/cm^2)
Decarbonized cast iron	Air cooling (as forged)	HRC 40.0	99.2	—	2.1
	Annealing (800°C–30 min.) (furnace cooling)	HRB 86.0	53.0	12.7	3.0
	Quenching (850°C, Oil quenching) (600°C, lhr., Tempering)	HRC 36.0	63.3	—	2.8
	Austempering (850°C, 30 min.) (350°C, salt bath 10 min.)	HRC 37.5	107.0	—	6.2
	* Sintering, air cooling	HRB 87.0	56.0	—	0.7
**Cast iron	Sintering, air cooling		42.0		
	Parent cast iron (wrought)	HRB 83.5	18.0		0.45

* For comparison, 8 ton/cm^2, 1150°C, lhr, ρ = 6.6 g/cm^3.
** For comparison also.

course this powder can be used for sintering as well as powder forging. The mechanical properties of sintered product of decarbonized cast iron powder and cast iron powder are shown for comparison in this table.

From these results the strength and toughness of the product can be greatly improved by the powder forging. These seems to be a little superior to conventional nodular graphite cast iron in regard to mechanical properties. By comparison with the parent cast iron which has a tensile strength of 15 ~ 20 kg/mm^2, it can be seen that the effect of decarbonizing are extraordinarily large.

5. Metallurgical Observations

The microstructure of forged products under different heat-treatment conditions and the microstructure of decarbonized cast iron powder are shown in Fig. 7. On comparison of these structure, (a) and (b) ~ (e), it is observed that the graphite flakes have disappeared and are converted into spherical graphites. The matrix has been reconstructed with a fine and homogeneous structure without pores, and around the spherical graphites a typical bull's eye structure which appears in nodular cast iron is observed in (b). In the microstructure of annealed one (c), clear round graphites exist in the ferrite matrix. In the microstructure of forged product in austempering shown in (e), the matrix is a bainit structure and the stable residual austenite has been found in the matrix.

An inspection of these micrographs shows that the spherical graphite is considerably smaller than that of nodular cast iron. This may be one of the reasons why these properties are superior to those of nodular cast iron. The evidence that spherical graphites exist in the matrix are shown in Fig. 8. The specimen has been line-annalized by a scanning electron microscope and the black balls show carbon to be at its peak and silcon decreasing. Again, Fig. 9 is a microphotograph of annealed forged specimen with further multiplication by a scanning electron microscope, in which the spherical graphite can be seen clearly along with the grain boundary.

The mechanism of the nodularization of graphite is considered to be as follows [6]. Since the forged product has been kept at 1150°C for a long time, through sintering and reheating the defects or the powder boundaries in crystal have been converted from fibrous shapes into tiny spherical cavities. Carbon atoms diffuse into the austenite matrix based on the presumptive (Fe-C-Si) constitutional diagram as illustrated in Fig. 10.

The diffusion coefficient of carbon atom is bigger than the self-diffusion coefficient of iron. These cavities are almost completely filled with graphite and remains as a graphite nodule at the time of cooling. Furthermore, the existence of 3.02% Si will accelerate the nodularization of graphite. During the eutectoid reaction, it will cause cementite to be decomposed and form Bull's eye structure around the spherical graphite.

6. Conclusions

(1) Extracting of graphite from cast iron powder can be easily and economically achieved with a cyclone machine by utilizing the difference of specific gravity between graphite and iron particles.

(2) Mechanical properties of powder forged products from

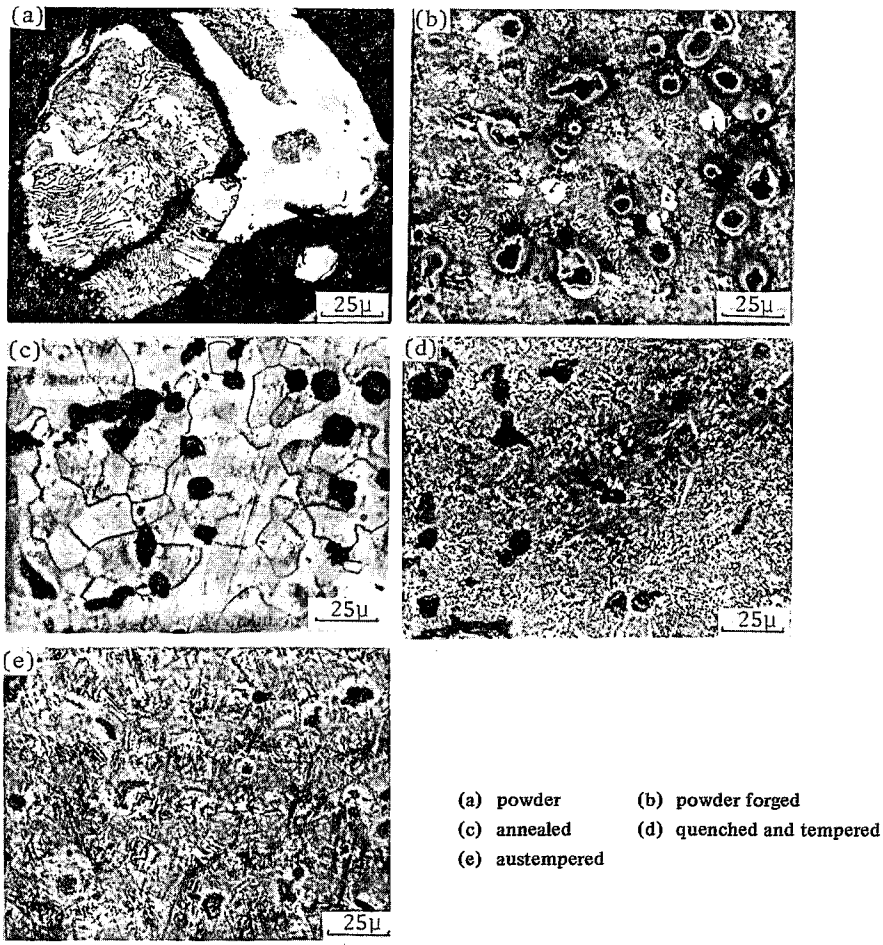

Fig. 7　Micrographs of powder and powder forged decarbonized cast iron.

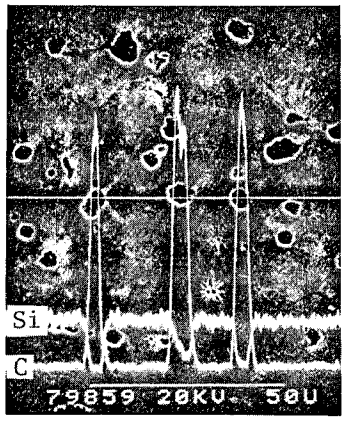

Fig. 8　X-Ray line analysis in the powder forged product of decarbonized cast iron.

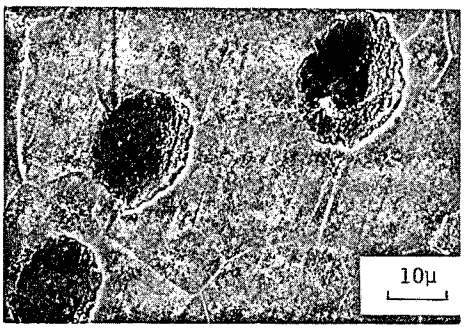

Fig. 9　Scanning electron micrograph of the powder forged product of decarbonized cast iron.

decarbonized cast iron powder are a little better than those of nodular cast iron and comparable to those of high carbon steel.

(3) These excellent properties come mainly from the conversion from graphite flakes existing in the powder into spherical graphite in the forged products.

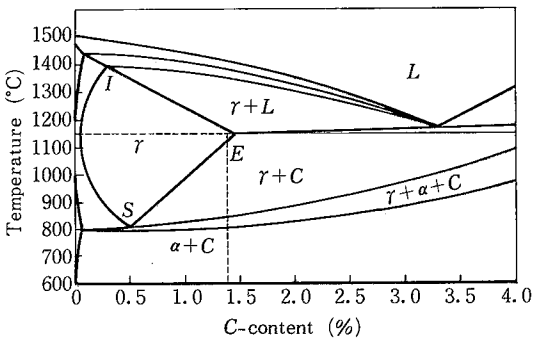

Fig. 10 Sliced phase diagram of Fe-C-Si (3%) alloy.

Acknowledgment

The authors are grateful to Brother Industries Ltd. For supplying swarf powder.

They also wish to extend their gratitudes to Dr. Takeuchi (The Tokyo Metropolitan Industrial Technological Center) and Mr. Ra (Seoul University) for their valuable assistances in this experiment. A part of this work was supported financially by the research fund of the Japanese Ministry of Education.

(Manuscript received, January 14, 1980)

References

1) T. Nakagawa, C.S. Sharma, T. Amano and M. Asano, Consolidation of cast iron machining swarf by sintering, Ann. CIRP, 24 (1) (1975) 197–201
2) T. Nakagawa, and C.S. Sharma, P/M forging and sintering for the recycling of machining swarf, Mod. Dev. Powder Metall. 9 (1977) 347–388
3) C.S. Sharma and T. Nakagawa, Recent development in the recycling of machining swarfs by sintering and powder froging, Ann. CIRP, 25 (1) (1977) 121–125
4) R.J. Dower and D.R. Oakley, The utilization of mild steel machining swarf in hot forging. N.E.L. report No. 542
5) R.J. Dower and J. Houston, The utilization of machining swarf for the production of bar, NEL Report No. 554
6) H.Y. Ra, E.Takeuchi, T. Nakagawa and F.S. Dai, The nodularization of graphite in sintering and powder forging of decarbonized cast iron powder. Japan P/M Conference, Nov. 1979 (in Japanese)